ドローンを用いた九重火山における繰り返し空中磁気観測により見積もられた磁場時間変化について

#宇津木 充 [1]), 橋本 武志 [2)], 多田 訓子 [3)], 太田 豊宣 [4)], 吉川 慎 [1)], 井上 寛之 [1)]
[(1] 京大・理・火山研究センター,[(2] 北大・理・地震火山セ,[(3] 海洋研究開発機構 海域地震火山部門,[(4] テラテクニカ

Magnetic field temporal change estimated by repeated aeromagnetic observations at Kuju volcano using a drone.

#Mitsuru Utsugi[1)],Takeshi Hashimoto[2)],Noriko Tada[3)],Toyonobu Ota[4)],Shin Yosikawa[1)],Hiroyuki Inoue[1)]
[(1]Aso Vol. Lab., Kyoto Univ.,[(2]ISV, Hokkaido Univ.,[(3]IMG, JAMSTEC,[(4]Tierra Tecnica

In Kuju Volcano, continuous and repeated geomagnetic field observation had been carried out since the phreatic eruption in 1995, and significant magnetic field temporal changes have been observed around Mt. Iou. The apparent source location of this temporal change was estimated in the western side of Mt. Iou, depth of 300-400 m (Hashimoto et al.,2002).

At Kuju Volcano, high-density aeromagnetic observation was carried out in Dec. 2004, and Sep. 2019. In the aeromagnetic observation in 2004, the magnetic anomaly was observed using the manned helicopter. In this survey, an observation bird, which carries the magnetometer (Geometrics Inc., G858 optically pumped total field magnetometer) and GPS, was towed by the helicopter. The survey area is 2km x 2km around the Mt. Iou, with the average height of 150 m above the ground. In the case of the aeromagnetic observation in 2019, we used the drone aeromagnetic survey system with the potassium magnetometer developed by Tierra Tecnica Ltd., and survey area was EW 1 km x NS 2 km around the Mt. Iou with altitude of 1750 m from the sea level.

Using these aeromagnetic data, we tried to extract the temporal geomagnetic field change associated with the volcanic activity. To this end, we applied the method based on the generalized mistie control method proposed by Nakatsuka and Okuma, 2006, and successfully obtained the temporal changes during the period from Dec. 2004 and Sep. 2019. Furthermore, we estimated the location, depth, volume, and the shape of the magnetic source that caused this temporal change using 3D magnetic inversion method proposed by Utsugi, 2019.

In our presentation, we will present the detail of our observations, method for extracting the temporal change, and the results of our analysis.

九重火山では、1995 年の水蒸気爆発以来磁場連続及び繰り返し観測点が行われ、九重硫黄山西側の地下浅部 (数百 m) にソースを持つ顕著な磁場時間変化が観測されている。ところで九重火山では、2004 年 12 月に硫黄山周辺部において高密度な空中磁気観測が京都大学により実施された。この観測では、磁力計及び GPS を搭載した観測バードを有人ヘリコプターに曳航させ、硫黄山周辺の 2km x 2km の領域で上空（対地高度およそ 150m）から磁気異常（磁場全磁力）を観測した。

この 2004 年の観測時から現在までの磁場時間変化を検出する事を目的に、我々は 2019 年 10 月に硫黄山周辺でドローンを用いた空中磁気観測を実施した。本観測では（有）テラテクニカ社のドローン空中磁気測定システム GSMP35U-DR を用いて全磁力の測定を行った。この観測システムは、DJI 社製ドローン Matrice600pro に GEM system 社製ポタシウム磁力計 GSMP-35U を搭載させたもので、ドローンが発するノイズの影響を除去するため、磁力計センサーを約 2.5m 吊り下げ、サンプリング間隔 0.05 秒で全磁力測定を行った。なお位置情報には Matrice600pro 搭載の GPS による計測データを用いた。この観測システムを用い、2004 年の飛行航路のうち、硫黄山周辺の東西約 1km、南北約 2km の領域において、海抜高度 1750m の一定高度で空中磁気観測を行った。

この観測で得られたデータと 2004 年の観測データについて Nakatsuka and Okuma (2006) の拡張交点コントロール法を元にした解析手法でデータ解析を行った。この結果硫黄山上空で、硫黄山の北側で正、南側で負の時間変化が抽出された。この変化のセンス、振幅は地上観測の結果とも調和的なものであった。この解析結果を元に、時間変化の原因となるソースの位置、深さ、体積及び形状を磁場三次元インバージョンの手法 (Utsugi, 2019) を用いて見積もった。本発表では観測方法、及び観測データについて報告すると共に、データ解析の詳細について報告する。

Aeromagnetic survey of Nishinoshima volcano by using drone: the current situation and future outlook

#Noriko Tada[1)],Hiroshi Ichihara[2)],Masaru Nakano[1)],Mitsuru Utsugi[3)],Takao Koyama[4)],Tatsu Kuwatani[1)],Kiyoshi Baba[4)],Fukashi Maeno[4)],Akimichi Takagi[5)],Minoru Takeo[4)]

[(1]IMG, JAMSTEC,[(2]Nagoya University,[(3]Aso Vol. Lab., Kyoto Univ.,[(4]ERI, The University of Tokyo,[(5]Japan Meteorological Agency

Nishinoshima volcano in the Ogasawara (Bonin) island arc erupted in 1973-1974 for the first time since its discovery in 1702, and has intermittently erupted since November 2013. According to Iizuka et al. (1975), Nishinoshima volcano was formed after the last geomagnetic reversal event (~0.77 Ma) because all rocks obtained from Nishinoshima showed normal remnant magnetization. Eruption style changed from Strombolian activity to a violent Strombolian eruption in June 2020 (Yanagisawa et al., 2020). Unfortunately, there is no permanent observation network on or around the island, only satellites can periodically observe volcanic activities such as thermal anomalies of the island (Kaneko et al., 2019). The volcanic island offers an opportunity to study island-forming eruption processes (Maeno et al., 2016) and formations of continental crust (Tamura et al., 2019). Thus, we have approached these issues through magnetic anomalies of the island. The magnetic anomaly images obtained by satellites are very coarse, and we decided to measure total magnetic anomalies above the island by using the drone with the potassium magnetic sensor developed by Tierra Tecnica Ltd. (Tokyo, Japan).

The aeromagnetic surveys were conducted during the cruise of the Japan Meteorological Agency weather ship Keifu-Maru in June 2019, and covered an area of about 3 km x 3 km including the emergent part of Nishinoshima volcano. We extracted the magnetic anomaly induced by the magnetization structure from the observation data and estimated the magnetization structure from the anomaly by applying the 3D inversion (Utsugi, 2019), which combines L1 and L2 norm regularizations. We conducted a cross-validation procedure (e.g., Bishop, 2006) to simultaneously determine optimum values of a regularization parameter and a hyperparameter. We found that Nishinoshima volcano had an average magnetization of about 3.0 A/m and that two more strongly magnetized bodies existed as of 2019 beneath the volcanic vent at about 300 m below sea level and the northeast slope of the volcano at depths between 300 and 800 m below sea level. These features may represent large bodies of solidified magma of the previous eruptions in 1973-1974. This study demonstrated the utility of this relatively safe and inexpensive observation method and this data analysis method for investigating the magnetic structure of remote volcanic islands. Repeated future surveys of this type may enable us to monitor volcanic activities that affect the magnetization structure of volcanoes. Therefore, we will conduct aeromagnetic surveys using the same drone system during the cruise of Shinsei-Maru in January 2022 in order to compare magnetic anomalies and magnetization structures before and after the eruption style change.

Electric self-potential change before and during the 2018 phreatic eruption of Iwo-Yama Volcano, Kirishima Volcanic Complex

#Koki Aizawa[1], Dan Muramatsu[1], Takeshi Matsushima[1], Takao Koyama[2], Makoto Uyeshima[3]
[1]SEVO, Kyushu Univ., [2]ERI, University of Tokyo, [3]ERI, Univ. Tokyo

A small phreatic eruption occurred on 19 April 2018 at Iwo-Yama (or Io-Yama) Kirishima volcano complex, Japan. At the location 500m north of the eruption vent, magnetotelluric (MT) monitoring station (Aizawa et al., 2013) have recorded electric and geomagnetic fields before and during the phreatic eruption. We first report that significant electric self-potential change occurs simultaneously with precursory 'ground tilt with tremor', which started 5 minutes before the onset of the eruption. After the onset of the eruption, the steam effusion became significant, and the northward electric field dramatically increased. Approximately 5 minutes after the onset of the phreatic eruption, an explosion occurred with a cock's tail plume that emitted rocks and blackish ash. Soon after the explosion, the plume return to be steam dominant, and northward electric field also return to be normal level. The most plausible explanation of the electric filed change is electrokinetic origin caused by the groundwater movement. Based on the change in ground tilt and electric field, we propose that the electric field changes were all generated by the movement of shallow cold groundwater above the clay rich layer (Tsukamoto et al., 2018). The high temperature fluid intrusion, which caused 'ground tilt with tremor', promotes the boiling beneath the eruption vent, and subsequently gather the cold groundwater to compensate the vaporized water. Similar self-potential changes were also observed at the time without eruptions. Our data and interpretation suggest that shallow groundwater flow controls the preparation process and the occurrence of phreatic eruptions. Shallow groundwater flow can be monitored by electric self-potential.

References

Aizawa K., T. Koyama, M. Uyeshima, H. Hase, T. Hashimoto, W. Kanda, R. Yoshimura, M. Utsugi, Y. Ogawa, and K. Yamazaki (2013), Magnetotelluric and temperature monitoring after the 2011 sub-Plinian eruptions of Shinmoe-dake volcano, Earth Planets Space, 65 (No. 6), 539-550.

Tsukamoto K., Aizawa K., Chiba K., Kanda W., Uyeshima M., Koyama T., Utsugi M., Seki K., and Kishita T. (2018), Three-dimensional resistivity structure of Iwo-yama volcano, Kirishima Volcanic Complex, Japan: Relationship to shallow seismicity, surface uplift, and a small phreatic eruption, Geophysical Research Letters, 45, 12,821-12,828.
https://doi.org/10.1029/2018GL080202.

後生掛地熱地帯での自然電位分布の変遷

#坂中 伸也 [1)], 田表 主良 [1)], 坪江 桂吾 [1)], 崎山 律 [1)], 輪倉 光矢 [1)], 森脇 知哉 [2)], 多田 悠也 [3)]
[(1] 秋田大・国際資源,[(2] 日特建設,[(3] 日立建機

Changes of distribution of the self-potential at Goshogake geothermal area, Towada-Hachimantai National Park, northeast of Japan

#Shinya Sakanaka[1)],Shura Taomote[1)],Keigo Tsuboe[1)],Ritsu Sakiyama[1)],Koshi Wakura[1)],Tomoya Moriwaki[2)],Yuya Tada[3)]
[(1]International Resource Sciences, Akita Univ.,[(2]Nittoc Construction,[(3]Hitachi Construction

We have conducted SP (Self-potential) surveys at five times since November 2019 at Goshogake geothermal area. The area is in a part of Towada-Hachimantai National Park, northeast of Japan and located on the foot of the Akita-Yakeyama active volcano. Goshogake geothermal area has active fumaroles, mud pots, hot springs etc. So far, in order to investigate the subsurface hydrothermal structure, we have carried out geophysical prospecting including GPR (Ground Penetrating Radar), induction method by the instrument called GEM-2, and ERT (Resistivity method). We have found that GPR scatterings are outstanding at resistive zones beneath a survey line along the shore of the Ooyunuma hot pond and that characteristic subsurface conductivity distribution related to alteration by GEM-2.

The positive anomalies of SP in this area is appeared around Ooyunuma hot pond and along the series of hot springs like as Oname-Motome and Konya-jigoku. On the other hand the negative anomaly is appreciated at the area surrounding Oodorokazan. The positive anomalies of SP are in accordance with the geological alteration zones and the high temperature of 1 m depth.

The change of distribution of SP is inferred to include the seasonal change. Consequently we try to construct the time-change model of SP distribution with seasonal change. At first glance it is difficult to grasp the tendency of change of SP distribution but we can put up a model and can explain the outline of SP changes and predict the SP change in near future.

人工的に組み込んだ切込みを有する花崗岩への多点電気測定手法の応用

#鈴木 健士 [1)], 吉村 令慧 [1)], 山崎 健一 [1)], 大志万 直人 [1)]
[(1] 京大・防災研

Application of procedure for multi-point electrical measurement to dry granite containing artificially slit

#Takeshi Suzuki[1)],Ryokei Yoshimura[1)],Ken'ichi Yamazaki[1)],Naoto Oshiman[1)]
[(1]DPRI, Kyoto Univ.

The proper interpretation of electrical resistivity estimated through geo-electromagnetic observations requires a good understanding of the rocks' electrical properties. Previous studies have measured the resistivities of various rock samples (e.g., Brace et al., 1965; Coster 1948; Fuji-ta et al., 2004; Fuji-ta et al., 2007). On the other hand, the appearances of small-scale structures (e.g., fractures) in electrical resistivity in larger-scale electrical resistivity of the rock sample have not been clarified. It is easy to prepare rocks that contain small-scale structures such as fractures and to image the internal structures of the rocks using non-destructive methods such as X-ray CT scanning (e.g., Kawakata et al. 1999). If we can determine the internal structures of a given sample together with the bulk resistivity, we may be able to establish quantitative descriptions of electrical resistivity at different spatial scales by comparison.

In previous studies, as a basis for the electrical tomography of laboratory-scale rock samples (〜10 cm), we developed a procedure for stable, multi-point, electrical measurement on rock samples (Suzuki et al., 2021). This procedure was applied to measurements using a 40-electrode array, potential distribution on an intact dry granite (diameter 52 mm, height 100 mm) surface in response to an injected current was measured. Obtained potential distribution agreed well with that predicted by forward modelling. It demonstrated the robustness the new procedure in array measurements.

In this study, as the first step towards electrical tomography to the rock samples containing heterogeneous structures, we performed multi-point electrical measurement of dry granite (diameter 52 mm, height 100 mm) containing artificially slit. The slit with a thickness (〜2 mm) equivalent to that of the fracture generated by the compression test was included in the granite, and the potential distribution on the sample surface generated by a point current source was measured by 40 electrode arrays. The potential distribution, including the local potential changes caused by the slit, was measured, which was in good agreement with that predicted by forward modeling. From this, it was shown that thin planar structure in the rock sample can be detected by our procedure.

地球電磁気学的手法によって求められる地下の比抵抗を正しく理解するために、実験室での岩石比抵抗測定は重要である。これまでに岩石のバルク比抵抗測定が広く行われてきた（たとえば、Brace et al., 1965; Coster 1948; Fuji-ta et al. 2004; Fuji-ta et al. 2007 など）。一方で、ある領域の岩石比抵抗にそれよりも小規模な構造（たとえば、岩石中のフラクチャーなど）の比抵抗がどのように表れるかは十分に調べられていない。実験室では X 線 CT スキャンなどの非破壊計測手法による岩石の内部構造推定が可能なので（たとえば、Kawakata et al. 1999 など）、岩石の比抵抗構造を電気トモグラフィー測定などで決定できれば、その比抵抗構造と非破壊計測によって求まった内部構造の比較が可能になる。フラクチャーなどを含む岩石試料でこれを行うことができれば、様々なスケールの構造と比抵抗の関係を調べられる可能性がある。

これまでの研究では、岩石試料（〜10 cm）に対する電気トモグラフィー測定を実現するために必要な、岩石試料に対する多点電気測定手法を構築した（Suzuki et al., 2021）。我々はその手法を 40 個の電極アレイによる測定へ適用し、点電流の印加によって生じる無垢な乾燥花崗岩 (直径 52mm、高さ 100mm) 表面の電位分布の測定を行った。測定された電位分布はフォワードモデリングによって予測されたものとよく一致し、このことから電極アレイを用いた電気測定における本手法の堅牢性が示された。

本研究では、不均質構造を有する岩石試料への電気トモグラフィー測定にむけた第一歩として、人工的に組み込んだ切り込みを有する乾燥花崗岩 (直径 52mm、高さ 100mm) への多点電気測定を実施した。花崗岩には圧縮試験によって生じるフラクチャーと同等の厚さ (〜2mm) の切込みを組み込み、同試料へ点電流を印加した際に生じる試料表面の電位分布を 40 個の電極アレイで測定した。切り込みによって引き起こされた局所的電位変化を含んだ電位分布が測定され、それはフォワードモデリングによって予測されたものとよく一致した。このことから、フラクチャーと同等の厚さを有する岩石中の薄い面状構造も本手法で検出可能であることが示された。

Introduction of a pilot Network-MT survey in the north island of New Zealand

#Makoto Uyeshima[1)],T. Grant Caldwell[2)],Maki HATA[3)],Yuki Obana[4)]
([1]ERI, the University of Tokyo,([2]GNS Science,([3]ERI, the University of Tokyo,([4]Engineering Science, Osaka Electro-Communication Univ.

Beneath the east coast of the North Island of New Zealand, westward subduction of the Pacific plate takes place. On the northern part plate interface, the slow slip earthquakes (or events, SSE) frequently occur. One candidate reason to explain the SSE (and not high-speed normal earthquake) occurrence is existence of interstitial fluids on the plate interface.

Electrical resistivity is a physical quantity which is sensitive to existence of interstitial water and, especially, to its connectivity. Therefore, if we can confirm temporal resistivity variation, where resistivity value reduces with enhanced connectivity on SSE occurrence, we will reinforce the hypothesis that the fluids cause the SSE occurrence.

Aiming at confirming such temporal structural variation associating with the SSE activities, we decided to perform the Network-MT survey in the northeastern coastal area of the North Island. In the target area, subduction angle is low, and the plate interface is located at depths of from 12 km to 20 km. Especially in the northern part of the east coast, SSE more frequently occur with recurrent interval of about 2 years. Thus, the target area is one of the best research fields to investigate temporal variation of the electrical resistivity structure with SSE occurrence in the world.

In the Network-MT surveys, copper telephone line network is used to measure the electrical potential difference between the electrodes. This enables us to measure the electrical potential differences using dipoles from several kilometers to 10s of kilometers length. The magnitudes of natural electric disturbances are much increased and integrated electric field data of high S/N ratio can be obtained. Very high S/N ratio measurements are needed to detect any temporal variation of the electrical resistivity associating with fluid transport near the plate interface.

In this presentation, we will describe our pilot Network-MT trial that commenced in December, 2019 at Tolaga Bay, about 40 km northeast of Gisborne. The survey was planned to evaluate feasibility of the Network-MT survey in the New Zealand. We will show observation configuration and discuss on quality and stability of the Network-MT response functions in the frequency domain between the electrical potential difference and the magnetic field.

東北地方のインダクションベクトルと虚部のインダクションベクトルについて

#市來 雅啓 [1)], 海田 俊輝 [1)], 小川 康雄 [2)]
[(1] 東北大院理,[(2] 東工大・火山流体

Attitudes of induction vector in NE Japan, and a character of quadrature phase induction vector

#Masahiro Ichiki[1)],Toshiki Kaida[1)],Yasuo Ogawa[2)]
[(1]Grad. School of Sci, Tohoku Univ.,[(2]VFRC, Titech

We had observed the electromagnetic field variation at about a hundred observation sites with an interval of 20 km in NE Japan for about 2 months, and obtained the in-phase and quadrature-phase induction vectors. The induction vector here is a Parkinson vector. We have reconfirmed the in-phase Parkinson vector nature of the strait effect by the Tsugaru Straits (Nishida, 1982 JGG) and the ocean effect caused by the Japan Trench. On the other hand, the quadrature-phase Parkinson vectors point outwards from the Kitakami belt at a period of 1280 seconds, and those of northern Akita prefecture, northern Iwate prefecture, and Aomori prefecture point northwards at a period of 7680 seconds. Bailey & Edwards (1976 Geophys. J. Roy astr. Soc.) studied induction vector in Great Britain and suggest that the in-phase induction vector reflects the coast effect, while the quadrature-phase induction vector reflects the geological structure inside the Earth. Supposed that the quadrature-phase induction vector reflects the structure inside the earth, the quadrature-phase induction vector at a period of 7680 seconds in the Tohoku region indicates the existence of high conductors beneath northern region of the Tsugaru Straits. The final goal of this study is to elucidate the behavior of the quadrature-phase induction vector of the Tohoku region, and this presentation reports the result of numerical simulation of the behavior of the quadrature-phase induction vector.

We consider a two-dimensional model including land-sea distribution and the uppermost mantle conductor beneath the land. The quadrature-phase induction vectors point in the direction of the ocean and the mantle high conductor depending on skin depth. The in-phase induction vector points to the ocean regardless of skin depth or period.

We considered another model imitating a rectangular island with the uppermost mantle conductor beneath it. The quadrature-phase induction vector points to the mantle conductor for long periods, while the quadrature-phase vector shows a pattern of avoiding the coastline in a medium period range. In the short periods, it was shown to point towards the ocean. The in-phase induction vector points to the ocean at all periods.

Considering from above model simulations, the quadrature-phase induction vector is less affected by the ocean than the in-phase induction vector, and is sensitive to the high conductor inside the earth. The next future problem is to consider the effects of seafloor topography to the quadrature-phase induction vector in NE Japan.

　東北地方において 20km 間隔での各観測点約 2 か月間の電磁場変動を観測し、信頼性の高い実部と虚部のインダクションベクトルを周期 20 秒から 10000 秒まで求めた。ここでのインダクションベクトルは、Parkinson ベクトルである。実部の Parkinson ベクトルは、津軽海峡の海峡効果 (Nishida, 1982 JGG) や日本海溝の影響とみられる海洋効果を再確認する結果となった。一方虚部の Parkinson ベクトルは周期 1280 秒で北上山地から外側に向かって放射状に指向する傾向と、周期 7680 秒で秋田県北部、岩手県北部、青森県の Parkinson ベクトルは北向きを示す傾向が得られた。Bailey & Edwards (1976 Geophys. J. Roy. astr. Soc.) は英国グレートブリテン島のインダクションベクトルについて、実部のインダクションベクトルは海陸境界を反映する一方、虚部のインダクションベクトルは島内部または地球内部の地質構造を反映することを示唆している。虚部のインダクションベクトルが地球内部の構造を反映しているとすれば、東北地方の周期 7680 秒の虚部のインダクションベクトルの傾向は津軽海峡以北の地球内部の高伝導体の存在を示唆している。本研究では東北地方の虚部のインダクションベクトルの振る舞いを解明することを最終目的とし、本発表では表層の海陸分布と地殻深部やマントル最上部の高伝導体を配置した単純なモデルに対しての虚部のインダクションベクトルの振る舞いを数値計算でシミュレーションした結果を報告する。

　2次元的なモデルで海陸分布と陸域下のマントルに高伝導体を与えたモデルでは、虚部のインダクションベクトルは表皮深度とほぼ連動するスケールで海洋とマントル高伝導体の方向を指向することが分かった。実部のインダクションベクトルは表皮深度に関係なく長周期まで海洋を指向する。

　直方体の離島を模した海陸分布に、離島の真下のマントル最上部に高伝導体を置いたモデルでは、虚部のインダクションベクトルは長周期においてマントル最上部の高伝導を指向し、中程度の長さの周期では海岸線を避けるパター

ンを示し、短周期では海洋を向くことを示した。実部のインダクションベクトルは全ての周波数において海洋を指向した。

　　上記のモデルシミュレーションからは虚部のインダクションベクトルは実部のインダクションベクトルより海洋に影響されにくく、地球内部の高伝導体を比較的良く捉えているようである。

　　次の考察としては、東北地方の海底地形の影響を考察することが課題である。

Three-dimensional electrical resistivity structure beneath the back-arc side of the southern Tohoku region

#Yoshiya Usui[1)],Makoto Uyeshima[2)],Hideaki Hase[3)],Hiroshi Ichihara[4)],Koki Aizawa[5)],Takao Koyama[6)],Shin'ya Sakanaka[7)], Tsutomu Ogawa[8)],Yusuke Yamaya[9)],Nishitani Tadashi[10)],Yasuo Ogawa[11)],Ryokei Yoshimura[12)],Shinichi Takakura[13)],Masaaki Mishina[14)],Morita Yuichi[15)]

[(1]Earthquake Research Institute, the University of Tokyo,[(2]Earthquake Research Institute, the University of Tokyo,[(3]Geothermal Energy Research & Development Co., Ltd.,[(4]Graduate School of Environmental Studies, Nagoya University,[(5]Institute of Seismology and Volcanology, Faculty of Science, Kyushu University,[(6]Earthquake Research Institute, the University of Tokyo,[(7]Faculty of Engineering and Resource Science, Akita University,[(8]Earthquake Research Institute, the University of Tokyo,[(9]Renewable Energy Research Center, Fukushima Renewable Energy Institute, AIST,[(10]Faculty of Engineering and Resource Science, Akita University,[(11]Volcanic Fluid Research Center, Tokyo Institute of Technology,[(12]Disaster Prevention Research Institute, Kyoto University,[(13]Geological Survey of Japan, AIST,[(14]Graduate School of Science, Tohoku University,[(15]Center for Integrated Volcano Research, NIED

M7-class historical earthquakes have occurred beneath the back-arc side of the southern Tohoku region (e.g., the 1804 Kisakata earthquake, the 1894 Shonai earthquake). Since aqueous fluids can significantly influence subsurface rocks' mechanical properties, including the shear fracture strength of seismogenic faults, imaging subsurface fluid distribution is essential to understand the earthquake generation process. In addition, there are some volcanoes (e.g., Chokaisan, Gassan, and Zaosan) in the back-arc and backbone range area of the southern Tohoku region. It is considered that the volcanic activities of the area are also related to the subsurface fluids. An effective approach for imaging the subsurface fluid distribution is conducting an electromagnetic induction survey that delineates the electrical resistivity structure, which is sensitive to the interconnected fluid in subsurface rocks. Thus, to investigate the relationship between the subsurface fluid and the seismic and volcanic activities beneath the back-arc area of the southern Tohoku region, we carried out magnetotelluric surveys around the area and estimated a subsurface electrical resistivity structure. To reveal resistivity structure, we first estimated the impedance tensor, the vertical magnetic transfer function, and the inter-station horizontal magnetic transfer function using the BIRRP code (Chave and Thomson, 2004). The estimated response functions show characteristic features that seem to be related to the volcanos and faults around the study area, although the response functions appear to be strongly affected by the difference of the near-surface resistivity between relatively resistive mountainous areas and the conductive plains and basins. We then performed inversion to image the three-dimensional electrical resistivity structure of the survey area from the estimated response functions. In the inversion, we used the three-dimensional magnetotelluric inversion code FEMTIC (Usui 2015; Usui et al. 2017) and incorporated both terrain undulation and land-sea distribution into a computational mesh. This presentation shows a preliminary result of the three-dimensional inversion analysis.

Electrical resistivity structure beneath the southern part of Tohoku, NE Japan, revealed by magnetotelluric (MT) survey

#Dieno Diba[1],Makoto Uyeshima[2],Masahiro Ichiki[3],Shinya Sakanaka[4],Makoto Tamura[5],Yoshiya Usui[1]
[1]ERI, U Tokyo,[2]ERI, U Tokyo,[3]Grad. School of Sci, Tohoku Univ.,[4]International Resource Sciences, Akita Univ.,[5]Hokkaido Research Organization, Research Institute of Energy, Environment and Geology

Following the 2011 great Tohoku earthquake, intense shallow earthquakes were observed at the Iwaki area, which is the fore-arc side of southern Tohoku, Japan. At the same time, high strain rate accumulation at the back-arc side which corresponds to the Niigata-Kobe Tectonic Zone (NKTZ) was observed before the Tohoku earthquake and continues to this day. In addition, prominent geothermal activities are distributed along the backbone range in the central part of the area. We are encouraged to study the mechanism of those crustal activities from the electrical resistivity structure. By combining the result with the seismic and geodetic data, the physical processes of those activities can be comprehensively understood.

We performed a four years wide-band MT campaign (2015-2018) that consists of 3 survey lines along an approximately NW-SE direction running across the southern Tohoku. For the first attempt, we revealed a 2D resistivity structure along the 2015 survey line. MT impedances were obtained using the BIRRP robust MT data processing code by Chave and Thomson (2004). In addition to that, we also estimated the Tippers and inter-station horizontal magnetic field transfer functions (HMTF), in which the spatial variation of the horizontal magnetic field among the stations is examined. To obtain the resistivity structure, we developed a two-dimensional inversion code that reproduces the apparent resistivity, phase, Tipper, and HMTF data. Some prominent features of the resistivity structure will be discussed in the presentation, as well as the comparison of our result to the previous studies and hypocenters around the study area.

阿蘇2014年マグマ噴火前後における地下比抵抗分布の推移

#石橋 桜 [1]，宇津木 充 [2]，南 拓人 [3]，井上 寛之 [2]
([1] 京大・理,([2] 京大・理・火山研究センター,([3] 神戸大理

Distribution of subsurface resistivity before and after the Aso 2014 magmatic eruption

#Sakura Ishibashi[1],Mitsuru Utsugi[2],Takuto Minami[3],Hiroyuki Inoue[2]
([1]Kyoto Univ.,([2]Aso Vol. Lab., Kyoto Univ.,([3]Kobe Univ.

Knowledge of the subsurface hydrothermal system of volcanoes leads to understanding the mechanisms of phenomena such as phreatomagmatic explosions. The purpose of this study is to estimate the changes in the state of the subsurface hydrothermal system of the first crater of Nakadake, Aso volcano, from the changes in the subsurface resistivity distribution. Kyoto University has conducted ACTIVE observation, a kind of electromagnetic survey method, around the Nakadake first crater. In this study, we estimate the resistivity changes beneath the Nakadake first crater from the data obtained from February 2013 to August 2015 including the period of the 2014 Aso magmatic eruption.

In this study, we obtained the subsurface resistivity by inversion based on the method of Minami et al. (2018) using the ACTIVE data. Around the Nakadake craters, ACTIVE observations were carried out 7 times from February 2013 to August 2015, including the period of the 2014 eruption spanning from November 2014 to May 2015. Using these data, we calculated the subsurface resistivity structure at each observation time and estimated the resistivity change by taking their differences. We also reanalyzed the data used by Minami et al. (2018).

In the inversion by Minami et al. (2018), a tetrahedral mesh reflecting the local topography is first created. We then divide the subsurface calculation domain into large blocks with the dimensions of about 300m x 300m x 100m and assign one model parameter, i.e. resistivity value, to each block respectively. The subsurface domain far from the crater zone is considered as a single block. This grouping reduces the number of unknown model parameters. The inversion calculation is done with the aim of minimizing the sum of the data misfit term, and the roughness term which determines the smoothness of the model. In the inversion, it is necessary to give an initial model, which is also used as the reference model. In our study, the calculation was carried out by 1) changing the initial model and 2) choosing whether to include the outermost block as an unknown model parameter in the inversion. First, we used the AMT resistivity model obtained from Kanda et al. (2018, JpGU) as the initial model. The resistivity model for each observation period was calculated by inversion of the data obtained from the repeated observations. It was found that the inversion result for January 2014 resulted in the lowest residual regardless of whether the outer block was included as a model parameter. This model was used as a reference model of our second inversion, and the results of four different inversion results were finally obtained, namely two initial models with or without the outermost block model parameter.

The differences in the calculation methods described in the previous section did not change the structure of the resultant resistivity significantly, although there were some trivial differences. We then chose the model obtained with the second initial model with inclusion of the outermost block model parameter as our optimal model, and focused on the subsurface structure zone between 500m and 850m above sea level just below the Nakadake first crater. 1) From February 2013 to January 2014, the resistivity decreased from shallow to deep zones just below the crater. 2) From January to August 2014, this low resistivity zone enlarged. 3) From August to November 2014, the resistivity increased in a region below the crater. 4) On the other hand, from November 2014 to August 2015, the resistivity continued to be higher in a wider region, but the amount of change was smaller than in the previous period, and on the west side of the first crater, a conspicuous zone with lower resistivity appeared. A possible interpretation of the resistivity changes described above is as follows; 1) Even during the quiet period with the crater lake, the gases and volcanic fluids rise through the crack and its components dissolve into the water in the aquifer. Thus, the resistivity became low below the first crater.

2) As the volcanic activity increases, the supply of gases and volcanic fluids increases, and 3) the magma rises just before the eruption, and as the result, the temperature and the vapor pressure of the groundwater increase. Then, bubbles of gas intermingled with groundwater. 4) After the magmatic eruption ended, temperature and the vapor pressure of the groundwater made gradient and the bubbles disappeared from outside, so groundwater became just low resistivity fluids.

In our presentation, we will present the details of our analysis, including the resistivity model obtained for each period, results of the sensitivity calculations, and in addition, we will talk about new observation.

火山の地下熱水系についての知見を得ることは、水蒸気爆発などの現象のメカニズムを理解することにつながる。本研究では、阿蘇火山中岳第一火口の 2014 年マグマ噴火前後における地下比抵抗分布の推移から、地下熱水系の状態変化を推定することを目的とする。京都大学では、阿蘇中岳火口周辺において電磁探査法の一種である ACTIVE 観測 (Utada et al. ,2007) を行っている。本研究では、2014 年噴火及びその前後の 2013 年 2 月〜2015 年 8 月の期間で得られた ACTIVE データから中岳火口地下の比抵抗変化を推定した。

本研究では、ACTIVE から得られた観測データを元に、Minami et al. (2018) の手法に基づいてインバージョンを行い、地下比抵抗構造を求めた。阿蘇中岳火口周辺では、2014 年マグマ噴火の期間 (2014 年 11 月- 2015 年 5 月) を含む 2013 年 2 月から 2015 年 8 月にかけて 7 度 ACTIVE 繰り返し観測が行われた。これらのデータを用い、各観測時期における地下比抵抗構造を個別に求め、それらの比較から比抵抗時間変化を推定した。尚、この計算では Minami et al. (2018) で求められた期間についても再解析を行った。

　Minami et al. (2018) によるインバージョンでは、初めに地形データを反映した四面体メッシュを作成する。その後、対象領域をブロックに分割し、各々のブロックに含まれる四面体をグルーピングし、同じグループに属す四面体が同一の比抵抗値を持つと仮定する。さらに火口よりも十分遠い領域は一つのブロックとして考える。これにより実質的な未知変数の数を減らす。インバージョン計算は、データと順計算結果の残差項と、モデルの滑らかさを決定するラフネス項の和を最小とすることを目的として計算した。この計算では最初にモデルベクトルの初期値を与える必要があるが、今回は、(i) どのモデルを初期モデルとして採用するか、及び、(ii) 一番番外側のブロックの比抵抗値 (以下、外側比抵抗値) に変化を許すか、の 2 点を変えた計算を行った。まず、初期モデルに、 Kanda et al. (2018, JpGU) による AMT 観測データを用いた 3 次元インバージョンから得られた比抵抗モデルを用いた計算を行った。7 回（2013/2、2014/1、2014/5、2014/8、2014/11、2015/2、2015/8）の繰り返し観測によって得られたデータをインバージョン計算し、各々の観測時期における比抵抗モデルを求めた。それぞれ外側比抵抗値を変化させた場合とさせなかった場合の両方について計算したところ、いずれについても 2014 年 1 月の計算結果が残差最小となった。これを参照モデルとして再度計算を行い、最終的に 4 通りの計算方法による結果を得た。

　前節の計算方法の違いによって、細かな違いはあるが大局的な構造は変わらなかった。今回は、外側比抵抗値の変化を許して得たモデルを参照モデルとして、外側比抵抗値を固定したインバージョンを再度行い、得られた結果を最適解と見做して解釈する。火口直下の海抜 500m から 850m の領域に注目して解釈する。⌧ 2013 年 2 月から 2014 年 1 月にかけては火口直下の深さ方向に広い領域で抵抗値が低くなった。⌧更に 2014 年 1 月から 2014 年 8 月にかけてこの低抵抗化領域が広がったことが分かった。⌧ 2014 年 8 月から 2014 年 11 月にかけては火口周りの広い領域で高抵抗化した。⌧これに対し 2014 年 11 月から 2015 年 8 月にかけては、広い領域で高抵抗化は継続するものの前の期間よりは変化量が小さくなり、第一火口の西側では逆に顕著な低抵抗化領域が現れた。これらの比抵抗変化は、以下のように解釈できる。⌧まず、火口湖の存在する静穏期であっても噴火に向けて火山性ガスや火山性流体がクラックを通じて上昇してきており、その溶存成分が帯水層の水に溶け込む事で火口直下の地下水が低抵抗化する。⌧この後活動度が高まるにつれてガス、火山性流体の供給量が増加し、⌧さらに噴火直前にマグマが上昇する事により地下の温度が高まる。これにより地下水の蒸気圧が上昇し溶けきれなくなったガスが気泡状に地下水中に混在する状態となる。⌧マグマ噴火が収束すると、地下の熱量が下がり、温度勾配ができることによって外側の方から気泡が消え、単なる高導電性流体となる。 本発表では、感度計算や新たな観測点の増設についても述べる。
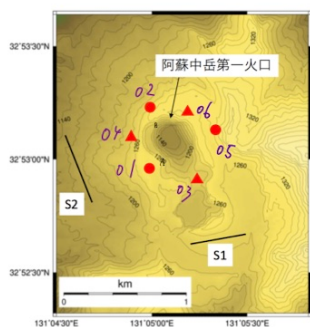

図２．ACTIVE観測点展開予定図．

広帯域 MT 法探査から推定される雌阿寒岳のマグマ供給系と浅部熱水系

#井上 智裕 [1)], 橋本 武志 [1)], 田中 良 [1)], 山谷 祐介 [2)], 市原 寛 [3)]
[(1] 北海道大学・理, [(2] 産総研, [(3] 名古屋大学・環境

The magma plumbing system and shallow hydrothermal system of Meakandake volcano inferred from broadband magnetotelluric survey

#Tomohiro Inoue[1)], Takeshi Hashimoto[1)], Ryo Tanaka[1)], Yusuke Yamaya[2)], Hiroshi Ichihara[3)]
[(1]Graduate School of Science, Hokkaido University, [(2]National Institute of Advanced Industrial Science and Technology,
[(3]Graduate School of environmental Studies, Nagoya University

This study reports an updated 3D resistivity model for Mt. Meakandake, one of the active volcanoes in eastern Hokkaido. On the northeastern foot of Mt. Meakandake, a remarkable ground inflation was observed during the period from 2016 to 2017 (Geospatial Information Authority of Japan, 2018). We modeled the 3D resistivity structure targeting at the inflation source, based on the BBMT data in 2018 and 2019 (Inoue et al., 2020; SGEPSS) and the AMT/BBMT data in 2010 recorded on the south shore of Lake Akan (Mogi et al., 2011). Our previous resistivity model has imaged a distinct conductive column C1 (about 1-10 Ω m) extending from 0.5 km BSL below the summit to a deeper part of Mt. Meakandake. We considered that C1 was likely to reflect a part of the magma plumbing system and volcanic conduit system of Mt. Meakandake. However, the geometry and spatial extent of C1 have not been well constrained by the lack of MT observation sites.

We measured the time series of five components (2E+3H) for about seven days using the ADU07e system (Metronix Ltd.) for the four sites in the western foot of Mt. Meakandake. On the summit area, we acquired only 2E using the Elog-dual recorder (NT System Design Ltd.). In calculating the response functions, we used the BIRRP (Chave and Thomson, 2004). Then, we performed a 3D resistivity inversion by ModEM (Egbert and Kelbert, 2012; Kelbert et al., 2014) based on the MT data (48 sites).

As the result of this inversion, the RMS misfit converged to about 3.2 with an error floor of 5 %, and a low resistivity body C1 (about 1 Ω m) extending from 0.5 km BSL just below Mt. Meakandake. This feature was similar to the previous model. The low resistivity layer Ca of about 5 Ω m was analyzed in the crater area, similar to the AMT 2D analysis by Takahashi et al. (2018). This low resistivity layer Ca deviated from C1 and appeared at about 0.5 km ASL.

We estimated the melt fraction using the modified Archie's law (Glover et al., 2000), assuming a magma reservoir. We estimated the resistivity of dacitic or rhyolitic melt from volcanic ejecta and calculated the bulk resistivity for different porosity. As the result, it was found that if the liquid phase was a rhyolitic melt, the bulk resistivity (1-10 Ω m) of C1 can be explained by the two-phase system of melt and rock.

The comparison of the shallow resistivity structure of the crater area and the distribution of volcanic earthquakes showed that the hypocenters near the Nakamachinesiri crater concentrated in the lower part of the shallow low resistivity layer Ca. This feature suggests that the low resistivity layer beneath the Nakamachinesiri crater reflects the layer altered by hydrothermal activity, and that volcanic earthquakes were occurring beneath the layer.

As a next plan, we plan to discuss the magma plumbing system and the shallow hydrothermal system of Mt. Meakandake using petrological information and drilling data.

　　北海道東部の活火山のひとつである雌阿寒岳の北東麓では，2016 年から 2017 年にかけて顕著な地盤膨張が観測された（国土地理院，2018）．我々は，この地盤膨張領域の地下構造に注目して，2018-2019 年に BBMT 観測を展開し，過去に阿寒湖畔で行われた AMT/BBMT（茂木・他，2011）データも用いて 3 次元比抵抗構造解析を行ってきた（井上・他，2020; SGEPSS）．これまでの解析結果によると，雌阿寒岳直下約 0.5 km BSL を上端とする柱状の明瞭な低比抵抗異常 C1（約 1-10 Ω m）が現れていた．我々は，この C1 が雌阿寒岳のマグマ供給系・火道系の一部を反映している可能性が高いと考えている．しかし，雌阿寒岳山頂域に観測点がなかったことから，C1 に対する制約は十分とは言えず，雌阿寒岳の火口域との構造的つながりも明らかでない．

　　そこで本研究では，雌阿寒岳山頂域 3 点と山麓 5 点に新しく観測点を置いた．西麓の観測には東京大学地震研の ADU07 と ADU07e（Metronix 社製）を使用し，電場 2 成分および磁場 3 成分のデータを取得し，BIRRP（Chave and Thomson, 2004）処理を行った．山頂域の 3 点では，Elog-dual（NT システムデザイン社製）で電場 2 成分のみを計測し，磁場については，同時計測した西麓観測点のデータを使用した．これらの新規データを加えた 48 地点の観測データを用いて，3 次元比抵抗インバージョン（ModEM, Egbert and Kelbert, 2012; Kelbert et al., 2014）を再度行った．

　　このインバージョンの結果，RMS misfit はエラーフロア 5 ％に対して約 3.2 まで収束し，井上・他（2020; SGEPSS）で報告した 3 次元比抵抗構造と大きく変わらずに雌阿寒岳周辺に約 0.5 km BSL から西に向かって深部に伸びる低比抵抗体 C1（約 1 Ω m）がこれまでの解析と同様に見られた．また，火口域には Takahashi et al. (2018) による AMT 法

2次元解析結果と同様な約 5 Ω m の低比抵抗層 Ca が現れた．この低比抵抗層 Ca は C1 の直上に乖離して現れていた．

　　C1 の実態に迫るために，マグマだまりと仮定して修正アーチー則（Glover et al., 2000）を用いてメルト分率推定を行った．デイサイト質メルトまたは流紋岩質メルトの比抵抗を火山噴出物から見積もり，空隙率を変えて bulk 比抵抗を計算した．その結果，液相が流紋岩質メルトならば，メルトと岩石の 2 相系で C1 の bulk 比抵抗（1〜10 Ω m）を説明できる可能性があることが分かった．

　　火口域の浅部比抵抗構造と火山性地震の震源分布を比較すると，浅部低比抵抗層 Ca の下部にナカマチネシリ火口付近の震源が集中する傾向が見られた．このことから，ナカマチネシリ火口直下の低比抵抗層は熱水によって変質した層を反映しており，その下部で火山性地震が発生していることが考えられる．

　　今後の予定として，岩石学的情報や掘削データを用いて雌阿寒岳のマグマ供給系と浅部熱水系の構造的関係について考察を深めていく．

胆振地方東部の MT 法地下比抵抗構造解析

#伊藤 凌 [1,3)], 橋本 武志 [2,3)], 井上 智裕 [1,3)], 上嶋 誠 [4)], 市原 寛 [5)], 山谷 祐介 [6)]
[(1] 北大院理,[(2] 北大・理・地震火山セ,[(3] 北大，理,[(4] 東大・震研,[(5] 名古屋大学地震火山研究センター,[(6] 産総研

Three-dimensional resistivity modeling in the eastern Iburi district, Hokkaido

#Ryo Ito[1,3)],Takeshi Hashimoto[2,3)],Tomohiro Inoue[1,3)],Makoto Uyeshima[4)],Hiroshi Ichihara[5)],Yusuke Yamaya[6)]
[(1]Grad. Sci., Hokkaido Univ.,[(2]ISV, Hokkaido Univ.,[(3]Sci., Hokkaido Univ,[(4]ERI, Univ. Tokyo,[(5]Nagoya University,[(6]FREA,
AIST

A magnetotelluric (MT) survey was carried out in October to November in 2018 at 14 sites around the epicenter of the 2018 Hokkaido Eastern Iburi earthquake (September 6, 2018: Mw 6.6). We inverted full components of the MT impedance and tipper to estimate a three-dimensional (3-D) electrical resistivity model of this area by using the BIRRP (Chave and Thomson, 2004) and ModEM programs (Egbert & Kelbert, 2012). The main shock was located at a depth of nearly 40 km, and its aftershocks were concentrated in a depth range from 20 to 40 km. It is important to investigate the subsurface structure of the seismogenic zone of such an unusually deep intraplate earthquake. Previous studies have suggested that the low resistivity regions in the mid-crust under active faults are saturated with aqueous fluid, and that pore water pressure increases as the fluid migrates to the surroundings, driving earthquakes (e.g., Ogawa et al., 2001). A distinct mid-crustal conductor was also found by Yamaya et al. (2017) beneath the Ishikari-teichi-toen fault zone (ITFZ), the western neighbor of the target area of our study. They presumed that the pore space created by ductile deformation of the lower part of the thick sediment layer was saturated with fluid. In our 3-D model a low-resistivity layer of about 10 Ω m was found at a depth from the surface down to c.a. 10 km. Similar conductive thick sediments were reported in the previous studies that dealt with the MT data across the Hidaka collision zone (Ichihara et al., 2019), and that investigated the ITFZ (Yamaya et al., 2017). On the other hand, in a depth range from 20 to 35 km, our 3-D model at present shows no distinct isolated conductor that is suggestive of saturated region. Instead, a slightly resistive zone of several hundred Ω m was imaged in the north of the hypocenter region. In the next step, we will incorporate the long period data obtained in 2021 into our inversion model to improve the sensitivity in the deeper part.

2018 年北海道胆振東部地震（Mw 6.6）（以下、胆振東部地震）の震源域周辺にて同年 10〜11 月に実施された MT 法観測データを解析し、BIRRP (Chave and Thomson, 2004) で求めたインピーダンス 4 成分とティッパー 2 成分を入力とする 3 次元インバージョン（ModEM: Egbert & Kelbert, 2012）で地下比抵抗構造を推定した。胆振東部地震は本震の震源深さが 40 km 近くにあり、余震の震源も深さ 20 km から 40 km に分布している。一般に内陸地震は深さ 5 km から 20 km 付近で発生することが多いが、胆振東部地震の震源はこれより深い位置に分布している。この特異性が地下構造に起因するものであるか否かを調べることは重要である。また、中部地殻にしばしば見られる低比抵抗域が流体に飽和した領域で、その流体が浅部に移動することで間隙水圧が上昇し、内陸地震が駆動されるとする先行研究がある（例えば，Ogawa et al., 2001 など）。本研究の対象地域西側に位置する石狩低地東縁断層帯の深部にも明瞭な低比抵抗体が発見されており、厚い堆積層の下部が延性的な変形を受けて生じた空隙に流体が飽和した状態にあると推定されている（Yamaya et al., 2017）。今回我々がここまでに解析した構造では、地下 10 km 以浅に 10 Ω m 程度の低比抵抗領域が見られた。日高衝突帯横断測線の MT データに基づく先行研究（Ichihara et al., 2019）や石狩低地帯で行われた上述の先行研究（Yamaya et al., 2017）でも、この地域の表層数 km は同様に低比抵抗となっており、厚い堆積層に対応していると考えられる。一方、現時点では、震源付近の北、深さ 20〜35 km に数百Ω m の相対的に高比抵抗な領域が現れているものの、この深度範囲には明瞭な低比抵抗異常は見られない。今後は、2021 年に実施した長周期帯の観測データも合わせてインバージョンを行い、より深部までの感度を高めた構造推定を行いたい。

弾性波探査およびボーリング調査結果を用いた阿寺断層帯主部南部の地下比抵抗構造の解釈

#伊藤 圭 [1]，壽山 美季 [2,6]，山口 覚 [1]，後藤 忠徳 [3]，加藤 茂弘 [4]，村上 英記 [5]
[1 大阪市立大学　理学研究科,[2 大阪市立大学　理学部,[3 兵庫県立大学　理学研究科,[4 人と自然博,[5 高知大学　自然科学系,[6 応用地質株式会社（現所属）

Interpretation of conductivity structure of the Atera fault, central Japan, with the results of seismic survey and borehole data

#Kei Ito[1],Miki Suyama[2,6],Satoru Yamaguchi[1],Tadanori Goto[3],Shigehiro Katoh[4],Hideki Murakami[5]
[1Graduate school of Science, Osaka City University,[2Faculty of Science, Osaka City University,[3Graduate school of Science, University of Hyogo,[4Museum of Human and Nature Activities, Hyogo,[5Natural Sciences Cluster, Kochi University.,[6OYO Corporation（Present address)

Surface and near surface structure of many active faults have been generally studied by geomorphological and geological surveys. Geophysical methods (seismic, electro-magnetic and gravity methods etc.) are useful to reveal subsurface structure of active faults.

The Atera fault zone in central Japan is one of the largest active faults in Japan and comprises the Sami, Shirakawa and Atera faults. The Atera fault is about 70km long, left-lateral and highly active (2-4m/1000yrs.) fault segment. Furthermore, some geophysical and boring surveys have been made around the fault. Therefore, it is possible to obtain reliable structure by combining multiple geophysical results. We further made an Audio-frequency Magnetotelluric(AMT) survey to add new constraint on the subsurface structure of this fault.

In this presentation, we show a newly determined resistivity model (ATR2021 model) and interpret subsurface structure around the Atera fault considering this model, borehole data and results of seismic survey.

An AMT survey was newly conducted at 8 stations in November 2020 in addition to 18 stations obtained at the 2019 survey. Magnetic reference station was operated at the point about 9km apart from the center of the survey line. MTU-5A systems (Phoenix Geophysics Ltd., Canada) were used at all stations.

MT impedances were determined according to the remote-reference processing procedure (Gamble et al., 1978), then they were subjected to dimensionality analysis using the phase tensor method (Caldwell et al., 2004; Bibby et al., 2005). The result shows that resistivity structure is two-dimensional, and its strike is N30 ° W-S30 ° E. The ATR2021 model along the model line (N60°E-S60°W) was determined using the two-dimensional magnetotelluric inversion code (Ogawa and Uchida, 1996).

The ATR2021 model has different features between northeastern and southwestern sides of the surface trace of the Atera fault. In the northeastern side, conductive region is widely recognized to a depth of 1,200m or more, in contrast, the southwestern side shows two-layer structure with a boundary depth of about 200m: shallower layer is conductive and deeper layer is resistive. These features are well consistent with the electrical and porosity logging data at two boreholes (Matsuda et al., 2008). Furthermore, these features are consistent with the results of the seismic survey. The upper boundary of the resistive layer in the southwestern side is well coincide with the remarkable seismic reflector. We interpret the boundary suggests the top of granitic basement. A flower structure exists near the surface trace of the Atera fault in the seismic section and a near-vertical resistivity boundary is clearly recognized below it. We interpret this resistivity boundary is the subsurface fault plane of the Atera fault.

　はじめに

　活断層の分布や活動履歴，変位速度，活動間隔などの地表付近の特性は，空中写真判読，変位地形や断層露頭の現地調査，トレンチ掘削調査などの地形・地質学的調査によって明らかにされてきた（e.g. 活断層研究会編,1991; Shirahama et al., 2016）．一方で，断層の地下形状や断層周辺の構造を明らかにすることも重要である．その方法として弾性波探査，重力探査，電磁気探査などの物理探査法がある（e.g. 岡田ほか, 2017; 山口ほか, 2016）．しかし，それぞれの探査法の特性が異なるので，地下構造を高い確度・精度で決定するためには，複数の物理探査法を組み合わせて総合的な解釈を行うことが望ましい（岡田ほか, 2018）．

　阿寺断層帯主部南部に位置する阿寺断層は長さ約 70km で，活動度の高い（2-4m/千年）左横ずれの活断層である．ここでは地形・地質学的調査（e.g. 遠田ほか, 1994; 山田ほか, 2012），ボーリング調査（Matsuda et al., 2008; 山田ほか, 2010）に加え，弾性波探査や重力探査 (地震予知総合研究振興会, 2002) 等の多様な調査が行われている．我々は，これまでほとんど未解明の地下比抵抗構造に着目し，Audio-frequency Magnetotelluric (AMT) 観測を行った．2019 年の観測に基づいた結果は，既に JpGU-AGU Joint Meeting 2020 で発表済みである．その後，より確度・精度の高い比抵抗モデルを得るため，2020 年に追加の観測を行った．

　観測

AMT 観測測線は，弾性波探査測線（地震予知総合研究振興会, 2002）にできるだけ沿うように設定した．2019 年に観測した 18 点に加え，2020 年には 8 点を新たに追加した．2019 年・2020 年ともに，AMT 測線中央から北西方向に約 9 ㎞離れた林（岐阜県加茂郡東白川村）に磁場参照点を設けた．いずれの観測においても MTU-5A（Phoenix Geophysics 社, カナダ）を用いた．

　解析
　各観測点で得られた磁場と電場の記録から，SSMT2000（Phoenix Geophysics 社, カナダ）を用いて，Remote reference 法 (Gamble et al., 1978) に基づき，南北および東西方向の MT 応答関数を算出した．モデル計算に先立ち，調査地域周辺の比抵抗構造の次元を Phase tensor 法 (Caldwell et al., 2004; Bibby et al., 2005) を用いて判定した．その結果，調査地域周辺の地下比抵抗構造は 2 次元であり，その走向は N30°W であると判断した．次に，Ogawa and Uchida (1996) のインバージョンコードを用いて，測線に沿う ATR2021 モデルを決定した．

　結果
　前モデルと比べて，領域を水平方向に約 1.2 ㎞拡大するとともに，モデル全体の，特に断層近傍および観測点間隔が広かった領域の確度・精度が向上した．ATR2021 モデルは，阿寺断層地表トレース付近を境に南西側と北東側で大きく様子が異なっている．
　北東側では，少なくとも深度 1,200 m まで低比抵抗領域が広がっている．南西側では，深度 200m までは低比抵抗領域が，それ以深では高比抵抗領域が存在している．これらの比抵抗領域の分布は，ボーリングデータから得られている比抵抗ログ，空隙率分布とも整合的である．さらにこのモデルは，弾性波探査の結果とも整合的である．特に南西部では，ATR2021 モデルの高比抵抗領域の上端と明瞭な地震反射面とが一致し，この地域の基盤をなす花崗岩類を反映していると考えられる．阿寺断層の地表トレース付近にフラワー構造が，その下位に比抵抗領域の高角な境界が存在し，これは阿寺断層の地下断層面を示唆している．また，城ヶ根山断層直下には非常に低比抵抗な領域が認められる．
　本発表では，阿寺断層帯主部南部の新しい地下比抵抗構造モデル（ATR2021 モデル）の特徴を述べるとともに，ボーリング調査結果および弾性波探査結果との比較について述べる．

山崎断層帯草谷断層の比抵抗構造

#乾 太生 [1,3], 山口 覚 [2], 伊藤 圭 [2], 壽山 美季 [1,4]

[1 大阪市大・理・地球, [2 大阪市大院・理・地球, [3 京都大学大学院 理学研究科 地球惑星科学専攻（現所属）, [4 応用地質株式会社（現所属）

Electrical conductivity structure of the Kusadani fault, the Yamasaki fault zone

#Taisei Inui[1,3],Satoru Yamaguchi[2],Kei Ito[2],Miki Suyama[1,4]

[1Department of Geosciences, Faculty of Science, Osaka City University,[2Geosciences, Graduate school of Science, Osaka City University,[3Division of Earth and Planetary Sciences, Graduate School of Science, Kyoto Univ.（Present address),[4OYO Corporation（Present address)

Introduction

The Yamasaki fault zone of southwest Japan is a typical left-lateral fault system southwest Japan that extends for 80 km with a general strike of N60 ° W-S60 ° E, and divide into the Nagisen fault zone, Main part of the Yamasaki fault zone and Kusadai fault. The Kusadani fault is located at the southeast end of the Yamasaki fault zone and is conjugate to the main part of the Yamasaki fault zone (The Headquarters for Earthquake Research Promotion, 2013; Hyogo Pref., 1999). The subsurface structure of this fault has been determined to a depth of only ˜4 m by trenching survey (Hyogo Pref., 1999). To clarify the relationship between the Kusadani fault and the main part of the Yamasaki fault zone in the future, we believe that information on the deep structure of the Kusadani fault is important. For this reason, aiming to reveal deep structure of the Kasadani fault, we conducted an Audio-frequency Magnetotelluric (AMT) survey across the Kusadani fault and to determine the two-dimensional (2-D) resistivity model to a depth of ˜1 km.

Observation

An AMT survey was undertaken at 11 stations in October 2020 along a transect (˜2 km) across the Kusadani fault. A reference station was set at ˜34 km NNW from the center of the transect. The MTU-5A (Phoenix Geophysics, Canada) systems were used at all stations.

Data analysis and Model analysis

MT response functions of each station was determined based on the Remote Reference method (Gamble et al., 1979) using SSMT2000 (Phoenix Geophysics, Canada). Next, we estimated the dimensionality of the resistivity structure beneath the study area and to determine the regional strike if the dimensionality were two-dimensional using the phase tensor analysis (Caldwell et al., 2004).

As a result, the resistivity structure is two-dimensional and its strike is N30 ° E-S30 ° W. Next, a two-dimensional resistivity structure model (KSD model) to a depth of 1.2km was determined using the code by Ogawa and Uchida (1996).

Result and Implication

The KSD model is characterized by three conductive regions, that is the deep conductor (C1), the shallow conductor (C2) and very shallow conductor (C3). The region C1 locates between 0.3 - 1.2 km in depth.

The region C2 is horizontal zone between 0.1 - 0.3 km in depth. The region C3 locates at 0.1 km in depth and spreads horizontally.

We interpret these regions as follows.

C1: Conductivity of the region is enhanced by groundwater in the damage zone formed by the fault activity of the Kusadani fault.

C2: Highly conductivity zone indicates the aquifer zone in basement rock.

C3: Highly conductivity zone indicates the aquifer zone in the overlying layer.

Region C1 can be interpreted as a fault zone conductor related to fault activity of the Kusadani fault. There are two possibilities for the location of the subsurface fault plane. One is a vertical plane beneath the surface fault trace of the Kusadani fault, and another is a plane along the upper boundary of the region C1.

はじめに

山崎断層帯は，兵庫県南部から岡山県東部に延びる活断層帯であり，北西から那岐山断層帯，山崎断層帯主部および草谷断層の３つの起震断層からなる（地震調査研究本部，2013）．那岐山断層帯には津山北方の断層と那岐山断層が，山崎断層帯主部には大原断層・土万断層・安富断層・暮坂峠断層・琵琶甲断層・三木断層が含まれる．草谷断層の一般走向は N58 ° E-S58 ° W であり，傾斜は地表近傍においてほぼ鉛直，北西側隆起の上下成分を伴う右横ずれ断層と報告されている（地震調査研究推進本部，2013；兵庫県，1999）．また，この断層は山崎断層帯主部と共役関係にある興味深い断層であるが，その地下構造はトレンチ調査（兵庫県，1999）によって深さ４m程度までしか求められていない．山崎断層帯主部との関係を今後明らかにするためには，草谷断層の深部構造の情報が重要であると考える．そのため本研究では，草谷断層の深部構造を明らかにすることを目的として Audio-frequency Magnetotelluric 法（AMT 法）観測を行い，深さ約 1 km までの比抵抗モデルの構築およびその解釈を行った．

観測

草谷断層の地表トレースに直交するように約 2 km の測線を設定し，この測線に沿う 11 地点で AMT 法観測を行った．また測線中央から北北西に約 34 km 離れた地点に磁場参照点を設けた．いずれの観測点においても測定には MTU-5A（Phoenix Geophysics 社，カナダ）を用いて，磁場 2 成分（南北，東西）と電場 2 成分（南北，東西）を測定した．

データ解析およびモデル解析

　観測で得られた磁場と電場データより，Remote Reference 法（Gamble et al., 1979）に基づき SSMT2000（Phoenix Geophysics 社，カナダ）を用いて，各観測点の MT 応答関数を算出した．各周波数の MT 応答関数を比較し，信頼度が高いと判断されデータのみを以降の解析に用いた．まず，Phase tensor 法（Caldwell et al., 2004；Bibby et al., 2005）を用いて，調査地周辺の比抵抗構造は 2 次元構造であり，その走向は N30°E-S30°W と判定した．次に，比抵抗構造の走向に直交するモデルラインに沿う 2 次元比抵抗構造モデル（KSD モデル）を求めた．モデル解析には ABIC 最小化による平滑化拘束付き 2 次元比抵抗構造インバージョンコード（Ogawa and Uchida, 1996）を用いた．

結果および解釈

　KSD モデルには，次の特徴的な 3 つの低比抵抗領域が認められる：深さ約 0.3〜1.2 km の低比抵抗領域（C1），深さ約 0.1〜0.3 km の低比抵抗領域（C2），および地表〜深さ約 0.1 km の低比抵抗領域（C3）である．これらの特徴的な低比抵抗領域を次のように解釈した．

C1：草谷断層の運動によって生じたダメージゾーンに地下水が侵入して形成された低比抵抗領域
C2：基盤岩中の帯水層を反映していると考えられる低比抵抗領域
C3：被覆層中の帯水層を反映する低比抵抗領域

　領域 C1 は草谷断層に関連した低比抵抗領域とみなせるが，断層面の位置については．断層地表トレースから領域 C1 の中央をほぼ鉛直横切るケースと領域 C1 の上部境界に沿うように存在する場合の 2 つの可能性が考えられる．

比抵抗分布からみた郷村断層帯の地下構造および**Fault zone conductor**の時間変化

#山口 覚[1)], 三村 明[1)], 加藤 茂弘[2)], 村上 英記[3)]
[(1] 大阪市立大学大学院理学研究科,[(2] 兵庫県立人と自然の博物館,[(3] 高知大学理工学部

Electrical conductivity structure of the Gomura fault zone, southwest Japan and time-variation of the fault zone conductor

#Satoru Yamaguchi[1)],Akira Mimura[1)],Shigehiro Katoh[2)],Hideki Murakami[3)]
[(1]Graduate school of Science, Osaka City University, Japan,[(2]Museum of Nature and Human Activities, Hyogo,[(3]Faculty of Science and Technology, Kochi University

The Gomura fault zone in the Tango Peninsula, southwest Japan comprises the Chuzenji (CZJ), Gomura (GMR) and Go-seiho (GS) faults. These active faults align some km apart and nearly parallel to each other in the granitic rock region under the same stress field. The 2.8-km GS is shortest with an extremely unclear geomorphological feature. During the 1927 Kita-tango earthquake, the GMR underwent a significant surface rupture but did not the CZJ, although both are clear left-lateral strike-slip faults. From the geologic, tectonic, and paleo-seismic background, we can consider this fault zone as a suitable target for comparing topographic features and subsurface conductivity structure.

We conducted audio-frequency magneto-telluric surveys at 27 stations along the line crossing all of these faults and determined the two-dimensional resistivity model (GMR2019 model) to a depth of ˜1.5km.

The GMR2019 model can be divided into three Areas (Area 1 - Area 3). Area 1 occupies the northeastern side and shows a typical resistivity structure of the Miyazu granite body which is almost unaffected by active faulting. In the Area 2 at the center, the CZJ and GMR faults locate at the northeastern and southwestern ends, respectively. A nearly vertical highly conductive zone was detected just beneath the surface trace of the GMR up to ˜1 km deep. In contrast, no remarkable conductive region was found below that of the CZJ. The GS locates in the Area 3 at the southwestern side and was interpreted as a secondary fault because of the small and shallow conductive zone and very unclear fault topography with almost no accumulative displacements.

はじめに

郷村断層帯は丹後半島 (京都府) に位置する活断層帯で，陸上部は郷西方断層，郷村断層，仲禅寺断層の3つの活断層で構成される（地震調査研究推進本部，2004；岡田・東郷，2000）．郷西方断層は断層長が2.8kmと非常に短く，横ずれ変位を示す地形も不明瞭である．郷村断層では1927年の北丹後地震の際に左横ずれを主とする顕著な地表地震断層が生じた．一方，仲禅寺断層では明瞭な河谷の左横ずれ屈曲が認められるものの，北丹後地震の際には活動しなかった．このように郷村断層帯には断層長，平均変位速度，最新活動時期など断層運動の特性が異なる断層が数km以内に近接し，並行して存在する．さらに郷村断層帯周辺は，ほとんどが花崗岩の岩盤からなるため，各断層の特性とそれらの地下構造を比較・検討するのに適している．

本断層帯の比抵抗構造については，すでに三村ほか（JpGU2017）で発表しているが，本報告では新たな解析結果と断層に関連した低比抵抗体の解釈について紹介する．

観 測

仲禅寺断層の約2km東から郷西方断層の約1.5km西までの約7kmの観測測線（2019Line）を設定し，この測線上で合計27点のAudio-frequency Magnetotelluric (AMT)法調査を行った（山口ほか，2016；三村ほか，2017）．データ解析にRemote reference法（Gamble et al., 1979）を用いるため，測線中央の観測点から約10km離れた地点Rに磁場参照点を設置し，水平磁場2成分（南北，東西）を測定した．いずれの測定にもMTU-5A（Phoenix Geophysics社，カナダ）を用いた．

解 析

データ解析には午前1時〜午前5時（JST）のデータを用いた．SSMT2000（Phoenix Geophysics社，Canada）を用いてRemote Reference法に基づき10,400〜0.35Hzの60の周波数において地理的南北および東西方向のMT応答関数を算出した．この時，No.3とNo.24を除く25点では地点Rの磁場を磁場参照データとして使用した．残りのNo.3とNo.24については，33Hzよりも高い周波数帯域では観測点相互を参照磁場点とし，それより低い周波数帯域では岩手県の国土地理院江刺観測場 (N39°14'12", E141°21'17")のMT連続観測データを磁場参照データとした．周波数選択を行ったのちPhase Tensor法（Caldwell et al., 2004；Bibby et al., 2005）で比抵抗構造の次元の判定を行い，Ogawa and Uchida (1996)のインバージョンコードを使用して2次元比抵抗モデル（GMR2019モデル）を決定した．

結果と考察

GMR2019モデルは5つの特徴的な低比抵抗領域（領域C1〜C5）の分布から，仲禅寺断層の北東側領域 (Area1)，仲禅寺断層と郷村断層が両端に位置する領域 (Area2)，郷村断層の北西領域 (Area3)の3つの領域に分けられる．

Area1は研究対象地域に広く分布する宮津花崗岩体の，郷村断層帯による活断層運動の影響をほとんど受けていない地質構造を反映していると解釈した．Area 2（中央部）には，郷村断層がその南西端に，仲禅寺断層がその北

東端に，それぞれ位置する．郷村断層の地表トレース直下には顕著な Fault zone conductor（FZC）が深さ 1km 付近まで認められ，これは郷村断層の活動に関連して形成されたと解釈した．一方，仲禅寺断層の地表トレース直下には FZC は認められなかった．両断層は同じ花崗岩体にあり，また同じテクトニックな環境にあることを考慮すると両者の FZC の違いは，両断層の活動休止からの経過期間の違い（郷村断層は約 100 年，仲禅寺断層は約 1 〜2 万年）に起因すると解釈した．Area3（南西部）には郷西方断層が存在する．この断層の地表トレース直下には深さ 300m 付近に顕著な低比抵抗領域 C1 が存在するが，それより深部は高比抵抗な領域となっている．北丹後地震時にも郷西方断層に沿っては地変は現れていない（岡田・松田，1997）．また，地表変位は郷村断層に比べて極めて不明瞭であることから，この断層は隣接する郷村断層の活動に伴って生じた副次的な断層であると解釈した．